Modeling of heat transfer in an industrial electric oven

Conference Paper · August 2013

1 author:

Chia-Wei Kuo
University of Wisconsin–Madison

Modeling of heat transfer in an industrial electric oven

Chia-Wei Kuo*, Yu-Cheng Liu, and Wen-Chey Chang

Energy Research Center, National Cheng Kung University, Tainan

Abstract

A case of industrial electric oven using solar source pre-heater to bake solar thermal absorption plates at 403 K was studied. It was found from the measurements that there were varying degrees of oven temperature variations (maximum 20 K) in the whole baking period, which would decrease the solar collection efficiency because of the plate bending phenomena. To find an effective method of solving, a validated 3D computational fluid dynamics (CFD) model was built in this paper. It was purposed to simulate the temperature profiles due to the conductive and convection heat transfer. Based on the modeling results, the problems were possibly resulted by the increasing heat loss phenomena at door slots due to the shortage of thermal insulation. Next, a modified oven design was proposed using the CFD model and coupled heating air of different motions. Compared with the earlier case, a better temperature distribution could be achieved.

Keywords：CFD; Heat transfer; Solar energy

1. Introduction

Solar energy was a competitive alternative for the decreasing fossil fuel supply in many countries [1-4]. For Taiwan ideally to develop solar thermal technologies due to the warm environment with hot summer [5], there was an increasing portion of domestic solar water heater installations over the last two decades [6]. Despite the popularization of this use, applications in pre-heating of industrial process were rather limited, because of the lack of product successfully developed.

Among various cases with problems to be solved, a heat transfer issue in an industrial electric oven was studied in this paper. The case was about the baking of 50 pieces of solar thermal absorption plates simultaneously at 403 K oven temperature, including using solar source pre-heater to reach 323 – 333 K. It was observed at the end of electric heating that there existed unacceptable temperature distribution variations at particular locations, which would result in the attenuations of solar collection efficiency, due to the plate bending phenomena. To find possible reasons for this problem, a 3D computational fluid dynamics (CFD) model was established in this paper. Based on the modeling results, a modified oven deign exhibiting better temperature distributions could also be suggested.

2. Oven heating mechanisms

The dimensions of oven were 2.46 m in length, 1.68 m in width and 2.37 m in height. Plates to be baked were located at x-z plane (the normal vector was parallel to y-axis). Two sets of doors were in the +x and +y directions. Enclosed by the +x door was a hollow cuboid with 15 circular holes as electric heating supply. Above that was the solar source pre-heater with 1 rectangular inlet. Each heating mode was accompanied by 1 forced square outlet. For the heating air patterns, it was shown in Fig. 1 (a) and (b).

(a)

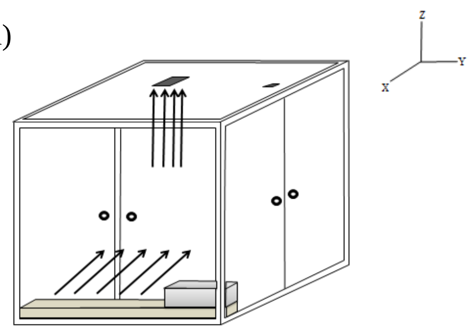

* Research assistant. Tel.: 06-3386501 ext. 215;
fax: 06-3386503; e-mail: phxiranter@gmail.com

(b)

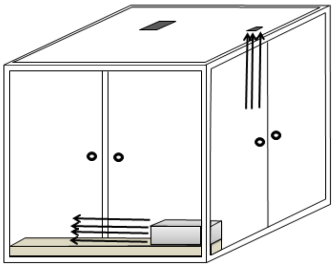

Fig. 1. (a) The air patterns of electric heating; (b) those of solar source pre-heater.

3. CFD simulation

To simplify the modeling problem, the number of plates contained in the baking process was reduced from 50 to 8. A numerical model was then built by the CFD code of ANSYS FLUENT v13.0 [7], with the unstructured 3D meshes of about 2.8 million hexahedral cells.

3.1 Modeling assumption

Due to the small spacing between each neighboring plates, the realizable k-ε model that allowed a straightforward implementation and not being computationally expensive [8], was used to model the possible turbulence characteristics of air flows. In addition, a steady state without the consideration of pre-heating mode was assumed. This was purposed to study the temperature profile when the energy supply and the heat loss were in balance at the end of baking [9].

3.2 Boundary conditions

At wall surfaces: A composite wall was used for achieving well insulation. It was based on the fiberglass of 21 mm thick, contacted by two layers of case iron each side. The overall heat flux including conduction and convection through the composite wall was given by Eq. 1.

$$q_w = U\left(T - T_a\right) \tag{1}$$

where U was the effective heat transfer coefficient of 1.18 W/m^2 k, calculated by Eq. (2).

$$U = \frac{1}{2/h_{iron} + L/k_{fiber}} \tag{2}$$

At door slots: In the industrial uses, the slots of doors were assumed to not have good insulation. Thus, a higher heat transfer coefficient than 1.18 W/m^2 was given.

At electric heating supply: The digital anemometer (Model AM-4203) of The LUTRON ELECTRONIC ENTERPRISE CO., LTD. was used to measure the inlet velocity of electric heating air. The averaging result of each individual hole (ϕ = 0.045 m) was 10.5 m/s and 4.3 m/s for the square outlet (0.186 x 0.186 m^2), with the measuring error of 2 %. To account for the inconsistency of total flow rate measured (inlet > outlet), which was resulted by the existence of solar outlet hole, the type of pressure outlet computed by Eq. (3) was used. For the input heating temperature, a constant of 403 K was given to approximate the steady state.

$$P_{dym} = \frac{1}{2}\rho v_{out}^{\ 2} \tag{3}$$

3.3 Governing equations

On the basis of 3D turbulence air flow at steady state, the heating air patterns within the oven were mathematically described by Eqs. (4) – (8) [10].

Mass conservation (Continuity equation)

$$\frac{\partial \rho}{\partial t} = -\left(\frac{\partial}{\partial x}\rho v_x + \frac{\partial}{\partial y}\rho v_y + \frac{\partial}{\partial z}\rho v_z\right) \tag{4}$$

Momentum conservation (Navier-Stokes equations)

$$\begin{aligned}\frac{\partial}{\partial t}\rho v_x = &-\left(\frac{\partial}{\partial x}\rho v_x v_x + \frac{\partial}{\partial y}\rho v_x v_y + \frac{\partial}{\partial z}\rho v_x v_z\right)\\ &-\left(\frac{\partial}{\partial x}\tau_{xx} + \frac{\partial}{\partial y}\tau_{yx} + \frac{\partial}{\partial z}\tau_{zx}\right) - \frac{\partial P}{\partial x} + \rho g_x\end{aligned} \tag{5}$$

$$\begin{aligned}\frac{\partial}{\partial t}\rho v_y = &-\left(\frac{\partial}{\partial x}\rho v_x v_y + \frac{\partial}{\partial y}\rho v_y v_y + \frac{\partial}{\partial z}\rho v_y v_z\right)\\ &-\left(\frac{\partial}{\partial x}\tau_{xy} + \frac{\partial}{\partial y}\tau_{yy} + \frac{\partial}{\partial z}\tau_{zy}\right) - \frac{\partial P}{\partial y} + \rho g_y\end{aligned} \tag{6}$$

$$\begin{aligned}\frac{\partial}{\partial t}\rho v_z = &-\left(\frac{\partial}{\partial x}\rho v_x v_z + \frac{\partial}{\partial y}\rho v_y v_z + \frac{\partial}{\partial z}\rho v_z v_z\right)\\ &-\left(\frac{\partial}{\partial x}\tau_{xz} + \frac{\partial}{\partial y}\tau_{yz} + \frac{\partial}{\partial z}\tau_{zz}\right) - \frac{\partial P}{\partial z} + \rho g_z\end{aligned} \tag{7}$$

Energy conservation

$$\rho C_P\left(\frac{\partial T}{\partial t}+v_x\frac{\partial T}{\partial x}+v_y\frac{\partial T}{\partial y}+v_z\frac{\partial T}{\partial z}\right)$$
$$=k\left[\frac{\partial^2 T}{\partial x^2}+\frac{\partial^2 T}{\partial y^2}+\frac{\partial^2 T}{\partial z^2}\right]$$
$$+2\mu\left[\left(\frac{\partial v_x}{\partial x}\right)^2+\left(\frac{\partial v_y}{\partial y}\right)^2+\left(\frac{\partial v_z}{\partial z}\right)^2\right] \quad (8)$$
$$+\mu\left[\left(\frac{\partial v_x}{\partial y}+\frac{\partial v_y}{\partial x}\right)^2+\left(\frac{\partial v_x}{\partial z}+\frac{\partial v_z}{\partial x}\right)^2+\left(\frac{\partial v_y}{\partial z}+\frac{\partial v_z}{\partial y}\right)^2\right]$$

With the specified boundary conditions, the governing equations were solved by the first-order upwind differencing scheme and the SIMPLE algorithm [11]. The 8000 iterations were found to give satisfactorily low residual for the variables to be obtained. The order of residuals was -7 for density and velocity, -9 for temperature, and -6 for k-ε model at the end of iteration.

3.4 Validation

Based on the thermocouple measurements of Model TC-CA-H(OS), it was observed that plates at Zone 3, as shown in Fig. 2, had the highest temperature distribution variations of 20 K. For the cases in Zones 1 and 2, the results were less than 10 K with higher average temperature similar to each other.

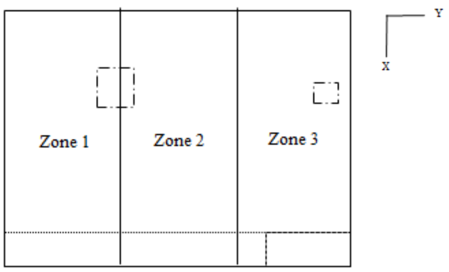

Fig. 2. Top-view of oven showing Zones 1 – 3.

Applying the experimental data, the CFD model with guessed heat transfer coefficients at door slots, could be corrected to give a satisfactory match to the measured temperature distribution trends.

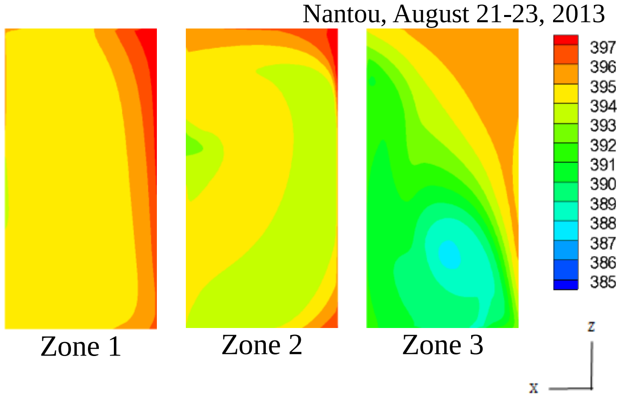

Fig. 3. Simulated temperature profiles (K) for plates at Zones 1 – 3.

With the modeling comparisons, the use of 5.9 W/m^2k for the lower part of door slot and 3.54 for the remaining was found to have the best match, as shown in Fig. 3. To further investigate the error, the measured data in Zone 3, which exhibited the highest variations, were compared against those of simulations. For the locations to be inspected, it was seen from Fig. 4.

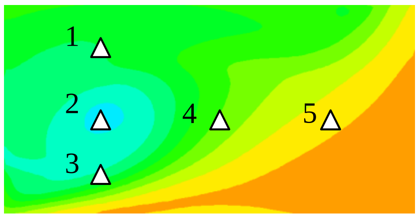

Fig. 4. The points to be observed in Zone 3.

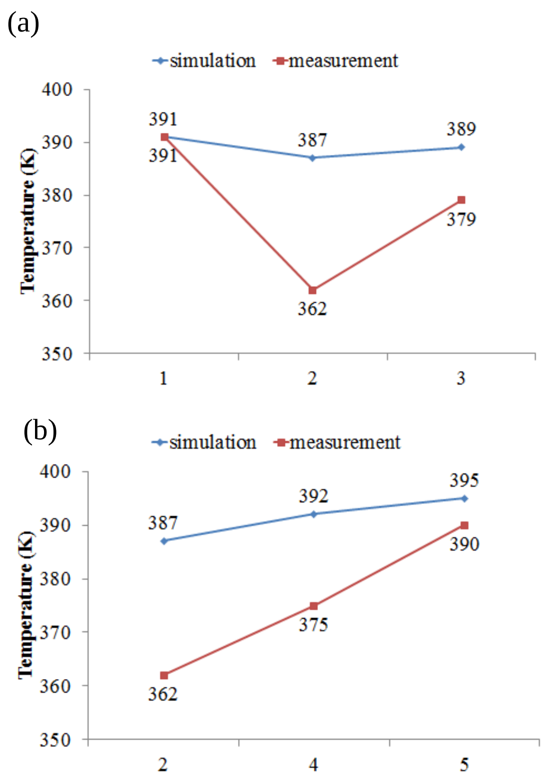

Fig. 5. (a) The simulation results with measured data overlaid, for points 1 – 3 of Fig. 4; (b) the points 2, 4, and 5.

As indicated by Fig. 5 (a) and (b), the modeling error was 14 % (in ℃ unit) relative to the measured data. This may be ascribed to the discrepancy between the theoretical estimation and experimental truth of effective wall heat transfer coefficient.

4. Modified oven design

With the CFD model validated, a modified oven design was capable of being proposed. Given the case comparisons of those of using differing heating mechanisms while keeping the original pump power of electric heating supply, the best performing design was suggested in Fig. 6. The temperature profile of plates in this case was shown in Fig. 7, where better temperature distributions with variation less than 7 K were observed.

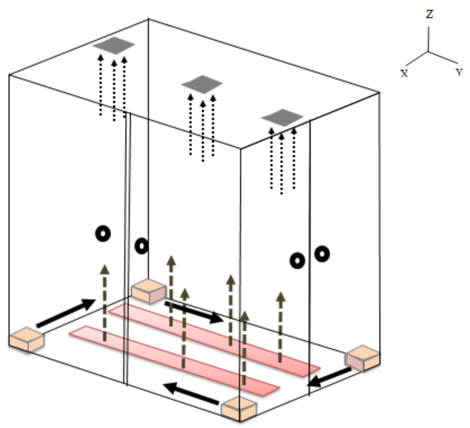

Fig. 6. The modified oven design

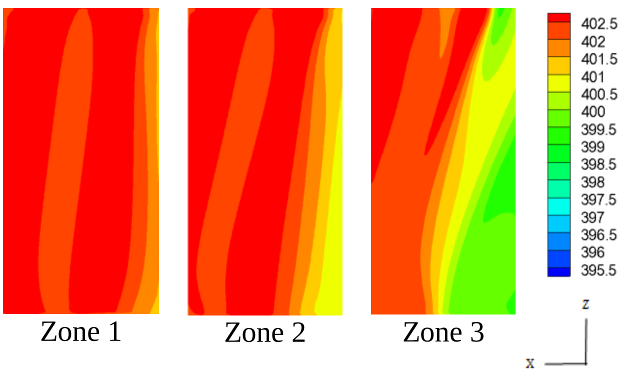

Fig. 7. The better temperature profiles (K) at Zones 1 – 3 using the modified design.

The modification used coupled heating air in vertical line (0.31 m/s) and horizontal circular (0.798 m/s) motions (Fig. 8 (a) and (b)), generated by the rectangular inlets at oven bottom (2.06 x 0.2 m^2 each one), and those at corners (0.2 x 0.1 m^2 each one), respectively. Since the air patterns between plates were the major concerns, a higher value of total flow rate from the bottom inlets was assumed. In the modified design, it was 4 times the amount of corner inlets. As for the outlet conditions, three squares (0.2 x 0.2 m^2 each one) were given at the oven top with equal state (0.9 pa). Note that for the purpose achieving the coupled heating air patterns, each inlet of Fig. 6 should include using the solar source pre-heater and electric heating supply.

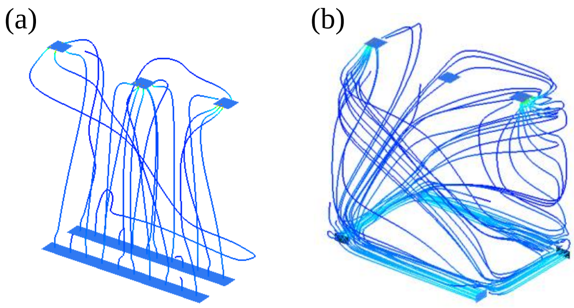

Fig. 8. (a) The air patterns in vertical line motions; (b) those in horizontal circular motions.

Although the dimensions of modified oven design were case-dependent, their availability in user-friendly concepts could provide a good knowledge about a better oven design to industrial uses.

5. Conclusions

A 3D steady-state CFD model was built in this paper, for investigating an industrial baking case which exhibited non-uniform temperature distribution. Based on the modeling comparisons against the measurements, it was ascribed to the increasing heat loss phenomena at door slots. Next, a modified oven design was suggested using coupled heating air of different motions via an aid of the CFD model. Compared to the earlier result, a better temperature profile with variation less than 7 K could be achieved.

Acknowledgements

This work was financially supported by the Bureau of Energy, the Ministry of Economic Affairs, Taiwan, Republic of China, under Grant No. 102 – D0304.

Nomenclature

C_P	specific heat (J/kg K)
g_x, g_y, g_z	gravitational acceleration (m/s^2) along x-, y-, and z-axis
h_{iron}	convection coefficient of cast iron (W/m^2 k)

k	thermal conductivity of air (W/m k)
k_{fiber}	thermal conductivity of fiber glass (W/m k)
L	length of fiber glass (m)
P	static pressure (N/m^2)
P_{dym}	dynamic pressure (N/m^2)
q_w	overall heat flux through the composite wall (W/m^2)
T	oven air temperature (K)
T_a	ambient air temperature (K)
U	effective heat transfer coefficient of the composite wall (W/m^2 k)
v_{out}	measured outlet velocity for the electric heating (m/s)
v_x, v_y, v_z	velocity on x-, y-, and z-axis (m/s)
μ	dynamic viscosity (Pa s)
ρ	air density (kg/m^3)
τ	viscous stress tensor
ϕ	diameter of electric heating inlet (m)

References

[1] Mirza, U. K., Maroto-Valer, M. M., and Ahmad, N., “Status and outlook of solar energy use in Pakistan”, Renewable and Sustainable Energy Review 7(6), pp 501-514, 2003.

[2] Jafar, M., “Renewable energy in the south pacific-options and constraints”, Renewable Energy 19(1), pp 305-309, 2000.

[3] Kalogirou, S., “Solar water heating in cyprus: current status of technology and problems”, Renewable Energy 10(1), pp 107-112, 1997.

[4] Haralambopoulos, D., Pararsenos, G. F., and Kovras, H., “Assessing the economic aspects of solar hot water production in Greece”, Renewable Energy 11(2), pp 153-167, 1997.

[5] Peel, M. C., Finlayson, B. L., and McMahon, T. A., “Updated world map of the Köppen-Geiger climate classification”, Hydrology and Earth System Science 11, pp 1633-1644, 2007.

[6] Chang, K., Lee, T., and Chung K., “Solar water heaters in Taiwan”, Renewable Energy 31, pp 1299-1308, 2006.

[7] Fluent 13.0: User’s Guide. ANSYS, Inc., 2011.

[8] Verboven, P., Scheerlinck, N., De Baerdemaeker, J., and Nicolai, B. M., “Computational fluid dynamics modelling and validation of the temperature distribution in a forced convection oven”, Journal of Food Engineering 43, pp 61-73, 2000.

[9] Therdthai, N., Zhou, W., and Adamczak, T., “Two-dimensional CFD modelling and simulation of an industrial continuous bread baking oven”, Journal of Food Engineering 60, pp 211-217, 2003.

[10] Bird, R. B., Stewart, W. E., and Lightfoot, E. N., Transport phenomena (2nd ed., 895 pp.). New York: John Wiley & Sons., 2002.

[11] Patankar, S. V. and Spalding, D. B., “A calculation procedure for heat, mass and momentum transfer in three-dimensional parabolic flows”, International Journal of Heat and Mass Transfer 15(10), pp 1787-1806, 1972.